

Accounting for Ground-Motion Spectral Shape Characteristics in Structural Collapse Assessment through an Adjustment for Epsilon

Curt B. Haselton, M.ASCE¹; Jack W. Baker, M.ASCE²; Abbie B. Liel, M.ASCE³; and Gregory G. Deierlein, F.ASCE⁴

Abstract: One of the challenges of assessing structural collapse performance is the appropriate selection of ground motions for use in the nonlinear dynamic collapse simulation. The ground motions should represent characteristics of extreme ground motions that exceed the ground-motion intensities considered in the original building design. For modern buildings in the western United States, ground motions that cause collapse are expected to be rare high-intensity motions associated with a large magnitude earthquake. Recent research has shown that rare high-intensity ground motions have a peaked spectral shape that should be considered in ground-motion selection and scaling. One method to account for this spectral shape effect is through the selection of a set of ground motions that is specific to the building's fundamental period and the site hazard characteristics. This selection presents a significant challenge when assessing the collapse capacity of a large number of buildings or for developing systematic procedures because it implies the need to assemble specific ground-motion sets for each building. This paper proposes an alternative method, whereby a general set of far-field ground motions is used for collapse simulation, and the resulting collapse capacity is adjusted to account for the spectral shape effects that are not reflected in the ground-motion selection. The simplified method is compared with the more direct record selection strategy, and results of the two approaches show good agreement. DOI: [10.1061/\(ASCE\)ST.1943-541X.0000103](https://doi.org/10.1061/(ASCE)ST.1943-541X.0000103). © 2011 American Society of Civil Engineers.

CE Database subject headings: Ground motion; Structural failures; Assessment; Spectral analysis.

Author keywords: Ground motions; Spectral shape; Epsilon; Collapse assessment; Performance assessment; ATC-63; FEMA P695.

Introduction and Goals of Study

One of the challenges in assessing structural collapse capacity by nonlinear dynamic analysis is the selection and scaling of ground motions for use in the analysis. Baker and Cornell (2005) have shown that spectral shape, in addition to ground-motion intensity, is a key characteristic of ground motions affecting structural response. In particular, for a given ground-motion hazard level (e.g., a 2% chance of exceedence in 50 years), the shape of the uniform hazard spectrum (UHS) can be quite different from the shape of the mean or expected response spectrum of a real ground motion having an equally high spectral amplitude at a single period (Baker 2005; Baker and Cornell 2006). Spectral shape characteristics are especially important for structural collapse assessments because at high amplitudes these differences are most significant. Therefore, when assessing the probability of collapse under

high-amplitude motions, the choice of ground motions significantly affects the collapse assessment.

To illustrate the distinctive spectral shape of rare ground motions, Fig. 1 shows the acceleration spectrum of a Loma Prieta ground motion. [The motion shown in Fig. 1 is from the Saratoga station and is owned by the California Department of Mines and Geology and included in the Pacific Earthquake Engineering Research Center (PEER) Next Generation Attenuation (NGA) database (PEER 2008). For this illustration, this spectrum was scaled by a factor of +1.4. This scaling is for illustration purposes only, and epsilons should be computed by using unscaled spectra.] The Loma Prieta spectrum has a rare spectral intensity at 1.0 s of 0.9 g, which has only a 2% chance of exceedence in 50 years. The figure also shows the mean expected spectrum predicted by the Boore et al. (1997) attenuation prediction that is consistent with the event magnitude, distance, and site characteristics associated with this ground motion. Fig. 1 shows that this extreme ground motion has a much different shape than the mean predicted spectrum. In particular, the spectrum for this record has a “peak” from approximately 0.6 to 1.8 s and lower intensities relative to the predicted spectrum at other periods. The intensity at 1.0 s, exceeded with a 2% likelihood in 50 years, is in the peaked region of the spectrum, and at this period the observed $S_a(1\text{ s}) = 0.9\text{ g}$ is much higher than the mean expected $S_a(1\text{ s}) = 0.3\text{ g}$; at other periods away from the peak, spectral values are closer to the mean expected S_a . This peaked shaped arises because ground motions that have an above-average intensity do not necessarily have equally large intensities at other periods.

At a 1.0 s period, the spectral value of the Loma Prieta record is 1.9 standard deviations above the predicted mean spectral value from the attenuation relationship so this record is said to have

¹Dept. of Civil Engineering, California State Univ. Chico, Chico, CA 95929.

²Dept. of Civil and Environmental Engineering, Stanford Univ., Stanford, CA 94305.

³Dept. of Civil, Environmental, and Architectural Engineering, Univ. of Colorado, Boulder, CO 80309.

⁴Dept. of Civil and Environmental Engineering, Stanford Univ., Stanford, CA 94305.

Note. This manuscript was submitted on October 13, 2008; approved on August 31, 2009; published online on October 2, 2009. Discussion period open until August 1, 2011; separate discussions must be submitted for individual papers. This paper is part of the *Journal of Structural Engineering*, Vol. 137, No. 3, March 1, 2011. ©ASCE, ISSN 0733-9445/2011/3-332-344/\$25.00.

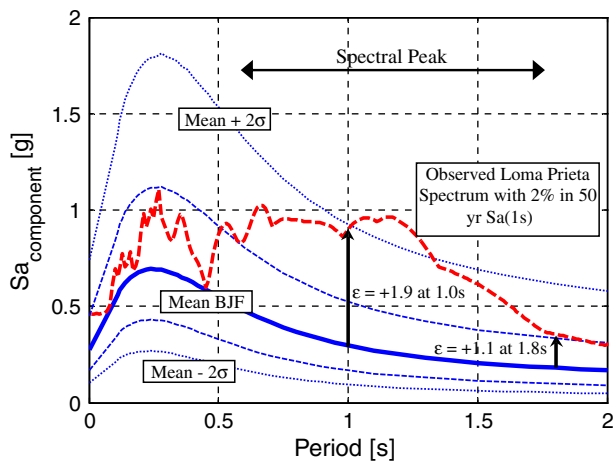


Fig. 1. Comparison of an observed spectrum from a Loma Prieta motion with spectra predicted by Boore et al. (1997); after Haselton and Baker (2006)

“ $\varepsilon = 1.9$ at 1.0 s.” ε (i.e., epsilon) is defined as the number of logarithmic standard deviations between the observed spectral value and the mean S_a prediction from a ground-motion prediction or “attenuation” model. Similarly, this record has $\varepsilon = 1.1$ at 1.8 s. Thus, the parameter ε is a function of the ground-motion record, the ground-motion prediction model to which it is compared, and the period of interest.

Just as ε is a function of the period, the relationship between ε and the spectral shape depends upon the period considered. For example, a motion with $\varepsilon(1 \text{ s}) = 2.0$ would tend to have a peak near a period of 1 s, and a motion with $\varepsilon(2 \text{ s}) = 2.0$ would tend to have a peak near a period of 2 s. Because ground motions are inherently random, this relationship between ε and the spectral shape (shown in Figs. 1 and 2) is not necessarily evident for individual ground motions, but is evident and statistically defensible when examining average trends in large data sets of recorded ground motions (Baker and Jayaram 2008).

The “peaked” spectral shape of rare ground motions observed in Fig. 1 is general to non-near-field sites in coastal California. In particular, such sites typically exhibit values of ε between 1 and 2 for the motions with a 2% in 50 years intensity levels. These positive ε arise from the fact that the return period of the ground motion (i.e., 2,475 years for a 2% in 50 years motion) is much longer than the return period of the earthquake that causes the ground motion (i.e., typical earthquake return periods that govern the high seismic hazard are 150–500 years in California). Accordingly, record selection for structural analyses at such sites should reflect the expectation of $\varepsilon = 1\text{--}2$ for 2% in 50 years motions.

This paper focuses on the consideration of the spectral shape through the parameter ε for the purposes of collapse assessment through nonlinear dynamic analysis. A prediction of structural collapse requires a set of ground motions in which the amplitude of each ground motion in the set is scaled to an increasing intensity until it causes collapse. The collapse capacity of an individual ground-motion record is denoted by the corresponding intensity on the basis of the spectral acceleration at the first-mode period of the building $S_{a,\text{col}}(T_1)$. The structure’s collapse capacity is then defined by the mean and dispersion of the collapse capacities of the individual records. [Strictly speaking, the “mean” used throughout this paper is defined as the geometric mean (i.e., the exponential of the mean of the logarithms). This mean is equal to the median of a lognormal distribution so it is also sometimes referred to as the “median.”] The proposed approach for selecting and scaling

records and characterizing spectral shape through the ε parameter is predicated on defining the ground-motion intensities by using $S_a(T_1)$.

As described subsequently, previous research has shown that the consideration of this peaked spectral shape significantly increases the computed collapse capacity of a structure relative to the results obtained by using motions without a peaked spectral shape. For cases in which these rare motions (i.e., those with ε values approaching 2.0) govern the performance assessment, such as when assessing the collapse risk of modern buildings in the seismic regions of California, properly accounting for the expected $+\varepsilon$ is critical.

The most direct approach to account for spectral shape in structural analysis is to select ground motions that have $\varepsilon(T_1)$ values that match the target $\varepsilon(T_1)$ obtained from a hazard analysis for the intensity level of interest, measured at the fundamental period of the structure. An alternative approach is to select and scale ground motions by an intensity measure other than $S_a(T_1)$, which accounts for a spectral shape in either an implicit or an explicit manner. Possible intensity measures include inelastic spectral displacement (Tothong 2007) or S_a values averaged over a period range (Baker and Cornell 2006). However, because the $S_a(T_1)$ intensity measure is widely used to describe the seismic hazard, the goal of this study is to develop an alternative approach to define and characterize the ground motions for analysis.

The proposed approach is intended to (1) permit the use of a general ground-motion set for structural analysis selected independently of ε values, and (2) then correct the collapse capacity estimates to account for the spectral shape. The correction adjustment is calculated by using $\varepsilon(T_1)$, which is computed for a given site and hazard level through the disaggregation of the seismic hazard for the site. Development of this proposed approach was motivated by related studies (FEMA 2008; Haselton and Deierlein 2007, chapters 6–7) that involved assessing the collapse safety of a large set of buildings with differing fundamental periods. Because of the large number of buildings and a desire to generalize the site characteristics as seismic design categories (SDC), selecting unique ground-motion sets for each of the buildings was not feasible.

This paper first discusses how the spectral shape and ε are related and then illustrates how the spectral shape affects the calculated structural collapse capacity. Next considered are the representative spectral shapes and the ε values expected for various sites and hazard levels. A regression method is proposed to account for the effects of the spectral shape on collapse by applying a correction factor to the mean collapse capacities obtained by using a generic ground-motion record set. The regression method is then applied to 111 buildings to develop a simplified method to adjust the collapse capacity through an ε correction factor.

Previous Research on the Epsilon Parameter and Spectral Shape Effects on Collapse Assessment

How Spectral Shape Relates to the Epsilon Values of Ground Motions

Fig. 1 shows the spectral shape of a single Loma Prieta ground-motion record that is consistent with a 2% in 50 years intensity level at 1.0 s and has $\varepsilon(1 \text{ s}) = 1.9$. This figure suggests that a positive ε value tends to be related to a peak in the acceleration spectrum around the period of interest. Recent studies have verified the statistical robustness of this relationship between a positive ε and a peaked spectral shape by using multiple ground motions. To illustrate, Fig. 2 compares the mean spectral shape of three

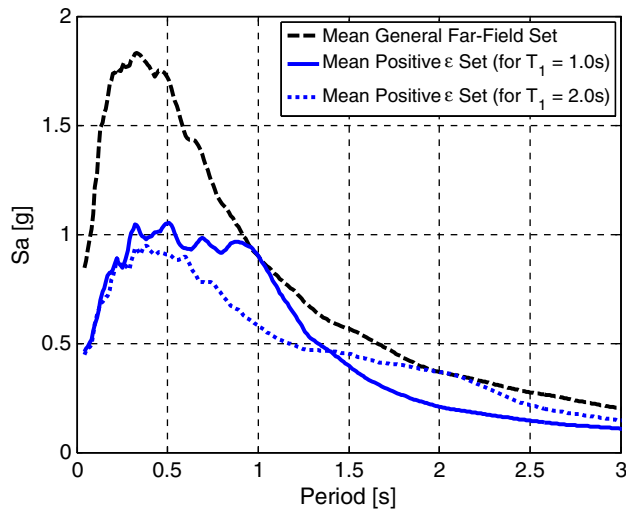


Fig. 2. Comparison of spectral shapes of ground-motion sets selected with and without considering ε after Haselton and Baker (2006)

ground-motion sets containing 78 motions, 20 motions, and 20 motions, respectively: (1) a set selected without regard to ε [i.e., general far-field set, described in FEMA (2008)], (2) a set selected to have $\varepsilon(1\text{ s}) = +2$, and (3) a set selected to have $\varepsilon(2\text{ s}) = +2$. The general far-field set is approximately epsilon-neutral. To facilitate comparison, the record sets were scaled such that the mean $Sa(1\text{ s})$ for Set 2 and $Sa(2\text{ s})$ for Set 3 were matched to the respective values of Set 1. Fig. 2 shows that the spectral shapes are distinctly different when the records are selected with or without regard to ε . When the records have positive ε values at a specified period, their spectra tend to have a peak at that period. This shape is much different than a standard uniform hazard spectral shape. Baker and Cornell (2005) developed a statistically rigorous method to predict this expected spectral shape, which is termed the conditional mean spectrum (CMS) because it is conditioned on an Sa value at a specified period.

How Spectral Shape (Epsilon) Affects Collapse Capacity

Selecting ground motions with peaked spectral shapes typical of rare ground motions, as represented by positive $\varepsilon(T_1)$ values, has been shown to significantly increase collapse capacity predictions for which capacity is defined $Sa(T_1)$. Conceptually, the difference in collapse capacity can be explained by comparing the spectral shapes of the epsilon-neutral set to the two positive epsilon sets anchored at 1.0 and 2.0 s. These sets are shown as long-dashed, solid, and short-dashed lines, respectively, in Fig. 2. For example, if a building period is 1.0 s and the ground-motion records are scaled to a common value of $Sa(1\text{ s})$, the spectral values of the positive epsilon set (represented by a solid line in Fig. 2) are smaller than those of the epsilon-neutral set (represented by the long-dashed line) for $Sa(T > 1\text{ s})$. The spectral values at longer periods are significant because the effective period will elongate as the structure becomes damaged. Similarly, the smaller spectral values for shorter periods (i.e., $T < 1\text{ s}$) for the positive epsilon set (represented by a solid line in Fig. 2) are significant because they will impact the contribution of higher modes with $T < T_1$.

Four studies have documented the effect of epsilon on nonlinear collapse simulations. Baker and Cornell (2005) studied the effects of various ground-motion properties on the collapse capacity of a 7-story nonductile reinforced concrete (RC) frame building with a fundamental period T_1 of 0.8 s. They found that the mean collapse capacity increased by a factor of 1.7 when an $\varepsilon(0.8\text{ s}) = 2.0$

ground-motion set was used in place of a set selected without regard to epsilon which had the mean $\varepsilon(0.8\text{ s}) = 0.2$. Goulet et al. (2007) studied the collapse safety of a modern 4-story RC frame building with a period of $T_1 = 1.0\text{ s}$ and compared the collapse capacities for a ground-motion set with a mean $\varepsilon(1.0\text{ s}) = 1.4$ to another set that had a mean $\varepsilon(1.0\text{ s}) = 0.4$. The set with $\varepsilon(1.0\text{ s}) = 1.4$ resulted in a mean collapse capacity that was 1.3–1.7 times larger than that of the $\varepsilon(1.0\text{ s}) = 0.4$ set in which the range was associated with variations in building design and modeling attributes. Haselton and Baker (2006) used a ductile, but degrading, single-degree-of-freedom oscillator with a period of $T_1 = 1.0\text{ s}$ to demonstrate that a $\varepsilon(1.0\text{ s}) = 2.0$ ground-motion set resulted in a 1.8 times larger mean collapse capacity compared to using a ground-motion set selected without regard to ε which had the mean $\varepsilon(1.0\text{ s}) = 0.2$. Likewise, Zareian (2006) investigated the effects that ε had on the collapse capacities of generic frame and wall structures. For a selected 8-story frame and 8-story wall building, he showed that a change from $\varepsilon(T_1) = 0.0$ to $\varepsilon(T_1) = 1.5$ resulted in a factor of 1.5–1.6 increase in mean collapse capacity.

The ε parameter has also been considered for the prediction of a response from near-fault ground motions but was found to not fully quantify the impact of forward-directivity velocity pulses on structural response (Baker and Cornell 2008). The approach proposed in this paper should not be applied to near-fault motions with large forward-directivity velocity pulses.

What Epsilon Values to Expect for a Specific Site and Hazard Level

Illustration of Concept by Using a Characteristic Event

To illustrate the relationship between expected ε , site, and hazard level, consider an idealized site in which the ground-motion hazard is dominated by a single characteristic event:

- Characteristic event return period = 200 years
- Characteristic event magnitude = 7.2
- Closest distance to fault = 11.0 km
- Site soil conditions— $V_{s30} = 360\text{ m/s}$
- Building fundamental period of interest = 1.0 s

Fig. 3 shows the predicted mean spectrum and spectra for mean ± 1 and 2 standard deviations (i.e., $\pm 1\varepsilon$ and $\pm 2\varepsilon$), given occurrence of the characteristic event. The mean predicted ground

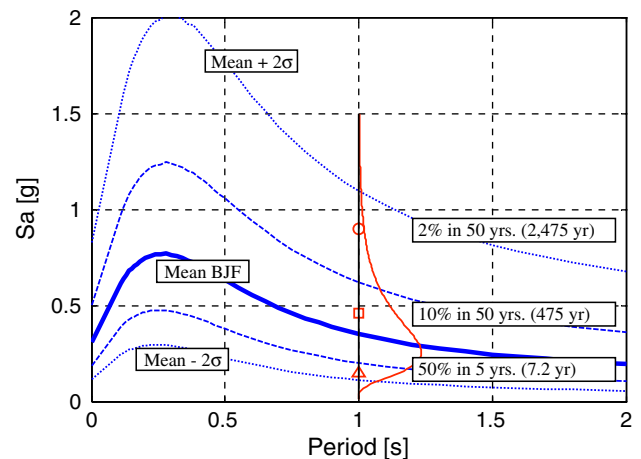


Fig. 3. Boore et al. (1997) ground-motion predictions for the characteristic event, predicted lognormal distribution at $T = 1.0\text{ s}$, and spectral accelerations for the 2% in 50 years and other hazard levels

motion is $S_a(1\text{ s}) = 0.40\text{ g}$ when using the Boore et al. (1997) attenuation model. This figure also includes a superimposed log-normal distribution of $S_a(1\text{ s})$ representing the predicted distribution of $S_a(1\text{ s})$ values, with a logarithmic standard deviation of 0.57, expected from an event with this magnitude and distance. The $S_a(1\text{ s})$ values associated with less frequent ground motions (i.e., 2% in 50 years) are associated with the upper tail of the distribution of $S_a(1\text{ s})$ for this event.

In general, when the return period of the characteristic earthquake (e.g., 200 years) is much shorter than the return period of the ground motion of interest (e.g., 2,475 years), then the ground motion of interest will have a positive ε . This statement is easily illustrated for an idealized site. When a single characteristic event dominates the ground-motion hazard, the mean return period (RP) of the ground motion $S_a \geq x$ is related to the characteristic event as follows:

$$\frac{1}{\text{RP}_{S_a \geq x}} = \left(\frac{1}{\text{RP}_{\text{Characteristic Event}}} \right) [P(S_a \geq x | \text{Characteristic Event})] \quad (1)$$

The return period for a 2% in 50 years motion, computed by using the standard Poissonian occurrence assumption, is $P(S_a > x \text{ in time } t) = 1 - \exp(-t/\text{RP}_{S_a > x})$, where $t = 50$ years and $P(S_a > x \text{ in time } t) = 0.02$. This results in a return period, $\text{RP}_{S_a > Sa2/50}$, of 2,475 years. The return period of the characteristic event is 200 years. From Eq. (1) then, $(1/2,475 \text{ years}) = (1/200 \text{ years}) * (0.081)$. Only 8% of motions that come from the characteristic earthquake are at least as large as the 2% in 50 years motion. An 8% probability of exceedance corresponds to 1.43 standard deviations above the mean value, or $\varepsilon(1\text{ s}) = 1.43$. A change in site soil conditions would affect the predicted spectral accelerations because of the change in the attenuation prediction, but it would not change the ε value because the ratio of the return periods of the ground motion of interest and the return period of the earthquake would be unchanged. The situation is more complicated for realistic sites with more earthquake sources, but in general the ε value associated with a design S_a level does not change significantly when the site conditions are varied.

The expected ε value depends strongly on the return period of the ground motion of interest. Fig. 3 shows that a 10% in 50 years motion (i.e., a return period of 475 years) is associated with $S_a(1\text{ s}) = 0.46\text{ g}$ and $\varepsilon(1\text{ s}) = 0.3$. For a much more frequent 50% in 5 years motion (i.e., a return period of 7.2 years), $S_a(1\text{ s}) = 0.15\text{ g}$ and $\varepsilon(1\text{ s}) = -1.7$. For cases in which rare motions drive the performance assessment, such as with the collapse assessment of modern buildings, it is likely that the ground motion will fall into the “positive ε ” category.

Eq. (1) also shows that the expected ε value depends on the return period of the characteristic event. In coastal California, earthquake return periods of 200 years are common, but in the eastern United States, large earthquake return periods are longer. These longer return periods in the eastern United States will cause the expected ε values for extreme (i.e., rare) ground motions to be smaller.

Expected Epsilon Values from the United States Geological Survey

Unlike the idealized site considered in the preceding section, most locations have several causal earthquake sources that contribute significantly to the ground-motion hazard, as well as having more complex distributions of magnitude. For the general case, expected ε values must be computed by disaggregating the results of the seismic hazard analysis.

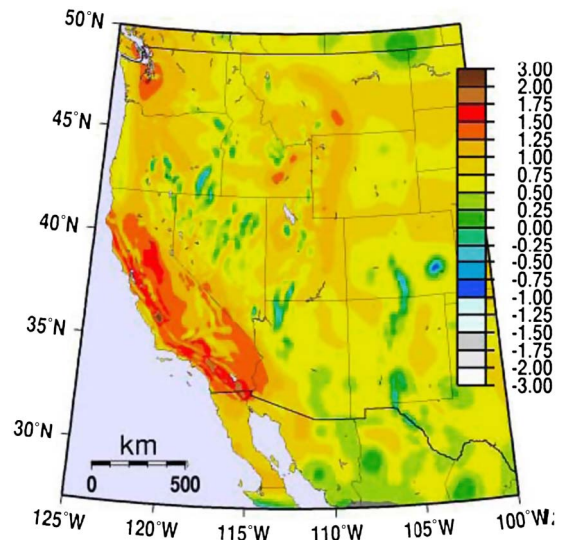


Fig. 4. Predicted $\bar{\varepsilon}_0$ values from disaggregation of ground-motion hazard, for the western United States in which the values are for a 1.0 s period and a 2% in 50 years motion after Harmsen et al. (2002)

The USGS conducted seismic hazard analyses across the United States and used disaggregation to determine the mean ε and $\bar{\varepsilon}_0$ values for various periods and hazard levels of interest (Harmsen et al. 2002; Harmsen 2001). Fig. 4 shows the $\bar{\varepsilon}_0$ for a 2% in 50 years $S_a(1\text{ s})$ intensity in the western United States for Site Class B (i.e., rock sites). Values of $\bar{\varepsilon}_0(1\text{ s}) = 0.50\text{--}1.25$ are typical in most of the western United States, except for the high seismic coastal regions of California, for which the typical values are $\bar{\varepsilon}_0(1\text{ s}) = 1.0\text{--}1.75$ with peak values as high as 2.0. In the eastern United States, typical values of $\bar{\varepsilon}_0(1\text{ s})$ are 0.75–1.0, with some values reaching up to 1.25, as shown in Fig. 5(a). Expected $\bar{\varepsilon}_0(1\text{ s})$ values fall below 0.75 for the New Madrid Fault Zone, for portions of the eastern coast, for most of Florida, for southern Texas, and in areas in the northwest portion of the map. The effect of period is illustrated by comparing Fig. 5(a) for $\bar{\varepsilon}_0(1\text{ s})$ to Fig. 5(b) for $\bar{\varepsilon}_0(0.2\text{ s})$, which shows that typical $\bar{\varepsilon}_0(0.2\text{ s})$ are slightly lower and more variable than $\bar{\varepsilon}_0(1\text{ s})$.

To further quantify the expected $\bar{\varepsilon}_0$ values in various regions of the United States, the numeric data used to create the described maps were examined. The data consists of expected $\bar{\varepsilon}_0$ values for periods of 0.2 and 1.0 s at the centroid of each zip code. Table 1 summarizes the subsets of these data for Seismic Design Categories B, C, and D, as defined by the International Building Code (2003). The table provides the average $\bar{\varepsilon}_0$ values and the spectral accelerations for four ground-motion hazard levels: 10, 2, 1, and 0.5% in 50 years for each SDC. The number of zip codes in each SDC, which is a general measure of building inventories, is also listed.

Because the fault characteristics on the western coast of the United States vary from those in other parts of the country (i.e., the recurrence intervals of the seismic events is shorter), Table 1 also shows the data for SDC D sites in California and in selected California cities. On average, the $\bar{\varepsilon}_0$ values are consistently higher in California when compared with other geographic locations of SDC D sites, and the $\bar{\varepsilon}_0$ values for many of the highly populated California cities are often even higher than the California average. For example, the $\bar{\varepsilon}_0(1\text{ s})$ value for the 2% in 50 years hazard in San Francisco is 1.5, whereas the average value for SDC D sites is 0.99. Values in Oakland, San Jose, and Riverside are even higher, ranging between 1.65 and 1.95.

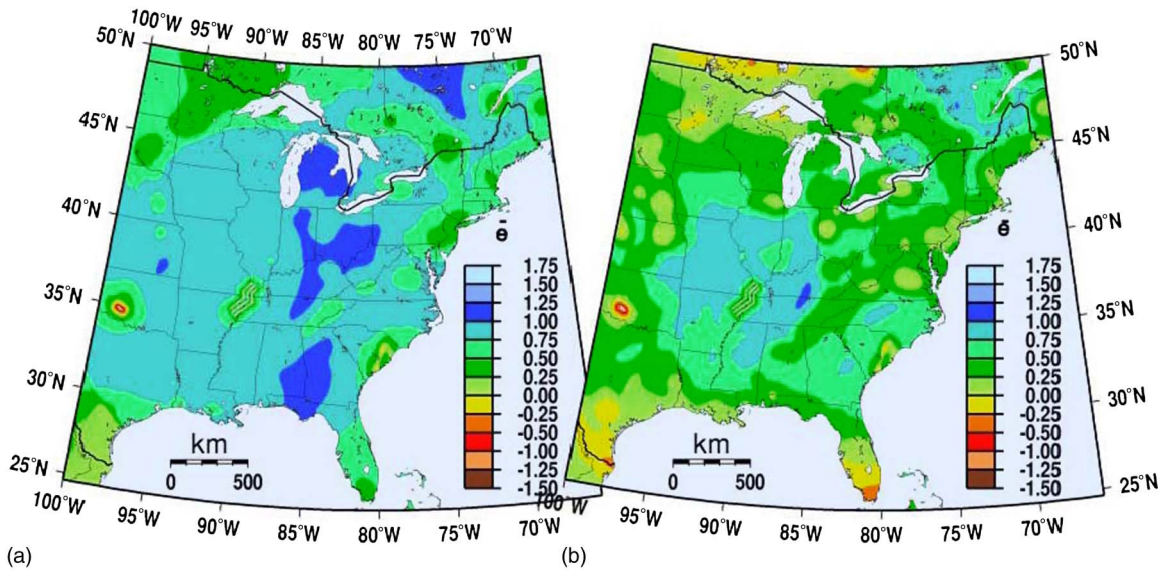


Fig. 5. Mean predicted $\bar{\epsilon}_0$ values from disaggregation of ground-motion hazard for the eastern United States in which the values are for (a) 1.0 s; and (b) 0.2 s periods and a 2% in 50 years motion after Harmsen et al. (2002)

Figs. 4 and 5, and Table 1 illustrate the expected $\bar{\epsilon}_0$ values for Site Class B (i.e., rock sites). These values should be generally applicable to other site conditions provided that the variability of the ground motions is similar to that of Site Class B. For Site Classes in which the variability in the ground motions differs from that of Site Class B (e.g., soft soil under very high levels of shaking), additional study is required to determine how the expected $\bar{\epsilon}_0$ values may vary from those for Site Class B.

Target Epsilon Values

The expected or target $\bar{\epsilon}_0$ value for use in a building response assessment depends on the site and hazard level of interest. Thus, the target ϵ should be determined on the basis of the hazard level that corresponds to the building performance level considered. For example, when computing the probability of collapse under a

ground motion with a 2% frequency of exceedence in 50 years, $P[C|S_a = S_{a_{2/50}}]$, the appropriate target hazard level is the 2% in 50 years intensity. When computing the mean annual frequency of collapse λ_{col} , the appropriate target hazard level is more difficult to determine. Ideally, one would increment the target $\bar{\epsilon}_0$ value for the various levels of S_a when integrating over the hazard curve. Alternatively, as an approximate approach, one could use the target hazard level that most significantly influences λ_{col} , which will be a function of both the site and the collapse capacity of the structure. Haselton and Deierlein (2007, chapter 5) looked at this question for two example 4-story RC frame buildings at a site in Los Angeles, and for those buildings and site, the ground-motion intensity level at 60% of the mean collapse capacity was the most dominant contributor to the calculation of λ_{col} . In their example, this corresponded to motions that have roughly 1.5 times the

Table 1. Mean Predicted $\bar{\epsilon}_0$ Values for Periods of 0.2 and 1.0 s, Sorted by Seismic Design Category, with Additional Detail Given for California Sites and Selected California Cities

Seismic design category	Average ϵ values								Average S_a values								Number Zip Code data points
	ϵ_0 (0.2 s)				ϵ_0 (1.0 s)				S_a (0.2 s) [g]				S_a (1.0 s) [g]				
	$\epsilon_{10/50}$	$\epsilon_{2/50}$	$\epsilon_{1/50}$	$\epsilon_{0.5/50}$	$\epsilon_{10/50}$	$\epsilon_{2/50}$	$\epsilon_{1/50}$	$\epsilon_{0.5/50}$	$S_{a10/50}$	$S_{a2/50}$	$S_{a1/50}$	$S_{a0.5/50}$	$S_{a10/50}$	$S_{a2/50}$	$S_{a1/50}$	$S_{a0.5/50}$	
SDC B	0.14	0.42	0.49	0.55	0.31	0.80	0.94	1.04	0.06	0.18	0.26	0.39	0.02	0.06	0.08	0.11	20,142
SDC C	0.11	0.51	0.63	0.75	0.23	0.74	0.88	1.00	0.11	0.31	0.46	0.66	0.04	0.10	0.14	0.19	7,456
SDC D	0.25	0.88	1.09	1.27	0.33	0.99	1.21	1.39	0.50	1.05	1.35	1.68	0.18	0.38	0.49	0.62	6,461
SDC D, CA	0.67	1.12	1.30	1.46	0.89	1.35	1.52	1.67	0.81	1.42	1.73	2.07	0.31	0.55	0.68	0.81	2,273
San Francisco, SDC D	0.88	1.57	1.79	1.95	0.75	1.50	1.75	1.94	1.13	1.78	2.07	2.37	0.52	0.89	1.07	1.25	16
Oakland, SDC D	0.75	1.50	1.75	2.00	0.95	1.65	1.89	2.13	1.56	2.60	3.07	3.55	0.60	1.01	1.21	1.41	10
Berkeley, SDC D	0.67	1.41	1.66	1.91	0.90	1.58	1.82	2.04	1.55	2.62	3.11	3.65	0.59	1.01	1.22	1.43	3
San Jose, SDC D	1.11	1.67	1.84	1.94	0.97	1.64	1.86	2.06	1.23	1.92	2.24	2.59	0.47	0.79	0.94	1.10	29
Los Angeles, SDC D	0.66	1.17	1.39	1.62	0.90	1.33	1.50	1.70	1.12	1.99	2.43	2.92	0.39	0.69	0.85	1.02	58
Riverside, SDC D	1.35	1.77	1.87	1.88	1.41	1.95	2.12	2.22	1.17	1.74	2.02	2.32	0.47	0.72	0.83	0.94	8

spectral acceleration of a 2% in 50 years ground motion and corresponding characteristic ε values typically larger than two.

Approaches to Account for Epsilon in Collapse Assessment

Two alternative methods of accounting for ε are illustrated by application to the collapse assessment of an 8-story RC frame model. The design and model were developed by Haselton and Deierlein (2007, ID 1011 in chapter 6) and consists of a three-bay special moment resisting perimeter frame (SMF) with 6.1 m (20 ft) bay widths, a tributary seismic mass floor area of 669 m² (7,200 sq ft), and a fundamental period T_1 of 1.71 s. Haselton and Deierlein (2007) provided more details regarding the nonlinear structural modeling and the methodology used for predicting collapse. The site used is in northern Los Angeles, is typical of the non-near-field regions of coastal California (Goulet et al. 2007), and has National Earthquake Hazard Reduction Program (NEHRP) Category D soil. The model's primary purpose was to compute the conditional collapse probability for a 2% in 50 years ground motion, which is $S_a(1.71 \text{ s}) = 0.57 \text{ g}$. Hazard disaggregation provides a target epsilon of $\varepsilon = 1.7$ for this level of ground motion.

Method 1: Ground-Motion Set Selected with the Target Epsilon

Select ground motions with ε values that are consistent with those expected for the site and hazard level of interest. When selecting records, we used the $\varepsilon(T_1)$ values computed with the Abrahamson and Silva (1997) ground-motion prediction equation. We selected a positive ε ground-motion set to include 20 ground motions having a mean $\varepsilon(T_1) = 1.7$ where $T_1 = 1.71 \text{ s}$ and each individual record has $\varepsilon(T_1) > 1.25$. We imposed additional selection criteria including both the minimum earthquake magnitude and the site class. Haselton and Deierlein (2007, chapter 3) documented the motions included in this ground-motion set and provided the complete list of selection criteria.

Fig. 6 shows the resulting collapse capacity distribution predicted by subjecting the 8-story RC SMF to the 20 ground motions of the positive ε set. The collapse capacity for a single ground-motion record is defined as the minimum $S_a(T_1)$ value that causes the building to become dynamically unstable, as

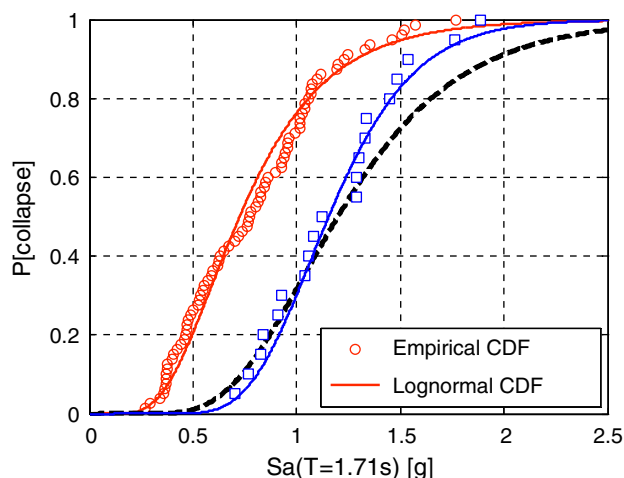


Fig. 6. Predicted collapse capacity distribution for the example 8-story reinforced concrete frame, computed by using the positive ε ground-motion set

evidenced by excessive drifts. This figure shows both the individual collapse capacities of the 20 records and a fitted lognormal distribution. The mean collapse capacity is $S_{a,col}(T_1) = 1.15 \text{ g}$, and the standard deviation of the logarithm of collapse capacities (denoted $\sigma_{LN(S_{a,col})}$) is 0.28. This dispersion, termed record-to-record variability, is associated with variation in ground-motion properties other than $S_a(T_1)$. For the 2% in 50 years $S_a(T_1) = 0.57 \text{ g}$, the conditional probability of collapse is quite low and equal to 0.5%.

Method 2: General Ground-Motion Set with Adjustments for Epsilon

Motivation and Overview of Method 2

Method 1 may not be feasible or practical in all situations, as it requires the selection of a specific ground-motion set for a specified period T_1 at a specified site with a target ε . For example, related work in the Applied Technology Council 63 Project (FEMA 2008) involved a collapse assessment of approximately 100 buildings, with differing fundamental periods, for generic seismic design categories. In such a study, the selection of a specific ground-motion set for each building is not practical; nor is it desirable because the goal is to generalize the collapse assessment results across seismic design categories.

Method 2 uses a general ground-motion set, selected without regard to ε values, and then corrects the calculated structural response distribution to account for the $\bar{\varepsilon}_0$ expected for the specific site and hazard level. This method can be applied to all types of structural responses (e.g., interstory drifts and plastic rotations), but this study focuses on the prediction of collapse capacity. Method 2 is outlined as follows:

1. Select a general far-field ground-motion set without regard to the ε values of the motions. These are termed the general set. The general set should have a large number of motions to provide a statistically significant sample and to ensure that the regression analysis in Step 3 is accurate.
2. Calculate the collapse capacity by nonlinear dynamic analyses, by using the incremental dynamic analysis method (Vamvatsikos and Cornell 2002) to scale records and organize the results in a cumulative distribution that is characterized by the mean and record-to-record dispersion of the collapse capacity.
3. Perform a linear regression analysis between the collapse capacity of each record $LN[S_{a,col}(T_1)]$ and the $\varepsilon(T_1)$ of the record. This analysis establishes the relationship between the mean $LN[S_{a,col}(T_1)]$ and the $\varepsilon(T_1)$ value.
4. Adjust the collapse capacity distribution, by using the regression relationship, to be consistent with the target $\varepsilon(T_1)$ for the site and hazard level of interest.

General Far-Field Ground-Motion Set and Comparison with Positive ε Set

The general set used in this study consisted of 78 strong far-field motions that were selected without consideration of their ε values. Haselton and Deierlein (2007, chapter 3) documented these motions and provided the complete list of selection criteria. A subset of 44 of these ground motions was also used in the "Applied Technology Council-63 (ATC-63) Project" (FEMA 2008) as part of a procedure to validate seismic provisions for structural design. The expanded set of 78 records was used to achieve more accurate regression trends between the collapse capacity and the ε values, but fewer may suffice. Fig. 7 compares the mean response spectra of the general set with the positive ε ground-motion record set described in Method 1. For comparison, both sets have been scaled

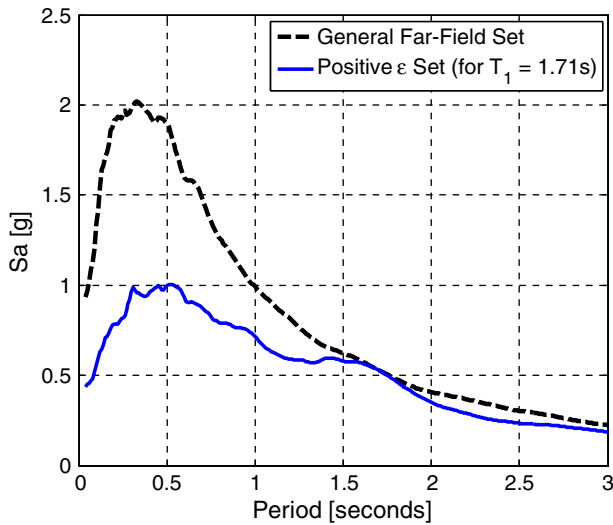


Fig. 7. Comparison of mean spectra for the general set and positive ε set of ground motion

so that each ground motion has the same $Sa(T_1) = 0.57$ g at $T = 1.71$ s. The peaked shape of the positive ε set, relative to the general set, is evident.

Application of Method 2 to Assess the Collapse of an 8-Story RC SMF Building

When subjected to the general set, the 8-story RC SMF building ($T_1 = 1.71$ s) has a mean collapse capacity $\mu_{Sa,col(T_1)}$ of 0.72 g and a dispersion in capacity of $\sigma_{LN(Sa,col)} = 0.45$. The 2% in 50 years intensity for this site is $Sa(1.71 \text{ s}) = 0.57$ g, so the probability of collapse for this level of motion is 29%. Recall that the probability of collapse under the 2% in 50 years motion when analyzed by using the positive ε set was only 0.5%. The collapse capacity prediction from the general set still needs to be adjusted to be consistent with the target $\varepsilon(T_1)$ for Method 2.

The collapse capacity $LN[S_{a,col}(T_1)]$ versus the corresponding $\varepsilon(T_1)$ values for each record are shown in Fig. 8. Also shown

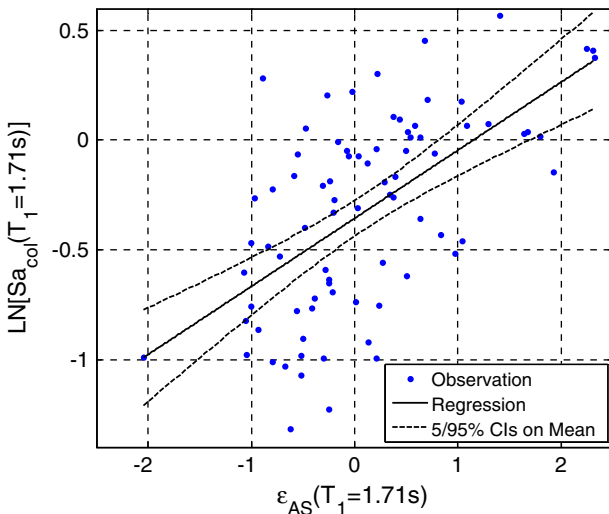


Fig. 8. Relationship between the collapse capacity quantified as spectral acceleration and ε for each ground-motion record computed by using Abrahamson and Silva (1997), including linear regression relating $LN[S_{a,col}(T_1)]$ to $\varepsilon(T_1)$

is a linear regression (Chatterjee et al. 2000) between $LN[S_{a,col}(T_1)]$ and $\varepsilon(T_1)$, which follows an approach previously proposed by Zareian (2006). The relationship between the mean of $LN[S_{a,col}(T_1)]$ and $\varepsilon(T_1)$ can be described as

$$\mu'_{LN[S_{a,col}(T_1)]} = \beta_0 + \beta_1 \cdot \varepsilon(T_1) \quad (2)$$

where $\beta_0 = -0.356$ and $\beta_1 = 0.311$ in this example. β_1 represents the slope between ε and the collapse capacity such that larger values of β_1 indicate a greater significance of ε in the prediction of the collapse capacity.

To adjust the mean collapse capacity for the target $\varepsilon(T_1) = 1.7$, Eq. (2) can be evaluated for the target $\bar{\varepsilon}_0(T_1)$, resulting in the following adjusted mean of $LN[S_{a,col}(T_1)]$:

$$\begin{aligned} \mu'_{LN[S_{a,col}(1.71 \text{ s})]} &= \beta_0 + \beta_1 \cdot [\bar{\varepsilon}_0(T_1)] \\ &= -0.356 + 0.311 \cdot [1.7] = 0.173 \end{aligned} \quad (3)$$

The adjusted mean collapse capacity can now be computed by taking the exponential of Eq. (3)

$$\text{Mean}'_{Sa,col(T_1)} = \exp(\mu'_{LN[S_{a,col}(T_1)]}) = \exp(0.173) = 1.19 \text{ g} \quad (4)$$

The calculation for the ratio of the adjusted to the original mean collapse capacity is

$$\text{Ratio} = \frac{\exp(\mu'_{LN[S_{a,col}(T_1)]})}{\exp(\mu_{LN[S_{a,col}(T_1)]})} = \frac{1.19 \text{ g}}{0.72 \text{ g}} = 1.65 \quad (5)$$

where $\mu_{LN[S_{a,col}(T_1)]}$ is computed directly from the collapse simulation results by using the general set of ground motions and $\mu'_{LN[S_{a,col}(T_1)]}$ is the value adjusted by the regression analysis for the target $\bar{\varepsilon}_0(T_1)$ value. The calculated increase in the mean collapse capacity from 0.72–1.19 g (a ratio of 1.65) has a significant impact on the collapse performance assessment.

The dispersion in the collapse capacity computed directly from the records is $\sigma_{LN[S_{a,col}(T_1)]} = 0.45$, but this capacity is also reduced by the adjustment to the target $\bar{\varepsilon}_0(T_1)$. The reduced conditional standard deviation can be computed as follows (Benjamin and Cornell 1970, Eq. 2.4.82):

$$\sigma'_{LN[S_{a,col}(T_1)]} = \sqrt{\{\sigma_{LN[S_{a,col}(T_1)],reg}\}^2 + (\beta_1)^2(\sigma_\varepsilon)^2} \quad (6)$$

where $\sigma_{LN[S_{a,col}(T_1)],reg} = 0.36$ is computed from the residuals of the regression analysis shown in Fig. 8, and σ_ε is the standard deviation of the $\varepsilon(T_1)$ values from disaggregation for a site and hazard level. For the example site used in this study, σ_ε is estimated to be 0.35 for the 2% in 50 years intensity of ground motion. Calculations for the reduced standard deviation in Eq. (7) show that the original record-to-record dispersion in collapse capacity (i.e., $\sigma_{LN[S_{a,col}(T_1)],reg}$) is more dominant than the effects of the dispersion in the expected ε value (i.e., $\sqrt{\beta_1^2 \sigma_\varepsilon^2}$)

$$\sigma'_{LN[S_{a,col}(T_1)]} = \sqrt{(0.36)^2 + (0.31)^2(0.35)^2} = 0.38 \quad (7)$$

The reduced dispersion is 15% lower than the dispersion in the collapse capacity computed directly from the records, which was $\sigma_{LN[S_{a,col}(T_1)]} = 0.45$. Relative to the increase in the mean collapse capacity described in the preceding, this decrease in dispersion from 0.45–0.38 has only a moderate impact on collapse performance assessment, which is most apparent near the tails of the collapse capacity distribution.

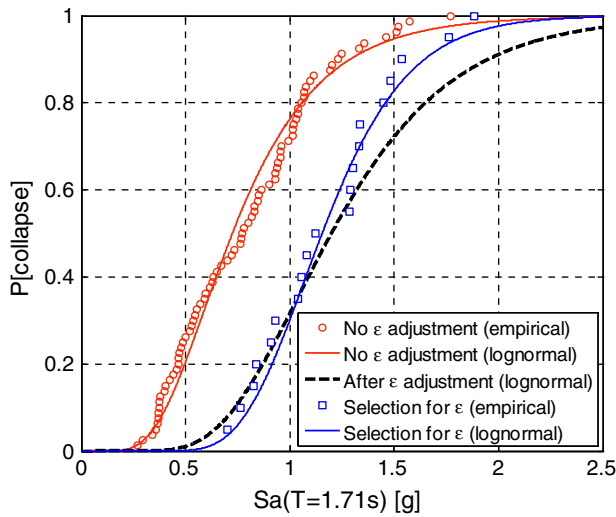


Fig. 9. Comparison of collapse capacity distributions predicted by using the two methods; Method 2 results are shown before and after the adjustment to the target $\bar{\varepsilon}_0(T_1)$

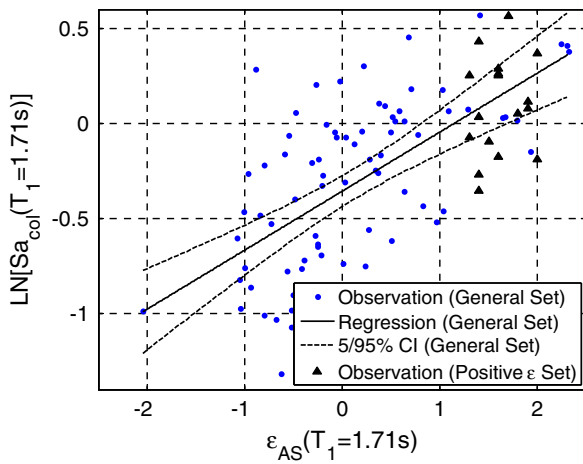


Fig. 10. Relationship between the spectral acceleration and ε from Fig. 8 including the collapse results predicted when directly by using the positive ε set of ground motions

Comparison of the Two Methods

Fig. 9 overlays the predicted collapse capacity distributions obtained from Methods 1 and 2 for the 8-story RC frame. The figure also includes the collapse predictions of Method 2 before the adjustment for ε . Fig. 10 is similar to Fig. 8, but for comparison, Fig. 10 includes the data for the positive ε set of ground motions. Together, Figs. 9 and 10, and Table 2 show that the two methods

produce nearly identical results, with the predictions of the mean collapse capacity differing by only 4%. The dispersion in the collapse capacity $[\sigma_{LN(Sa,col)}]$ differs from 0.28 for Method 1 to 0.38 for Method 2. From the writers' past experience, it is not expected that such a large observed difference occurs. The large difference in dispersion could be attributable to the smaller number of ground motions in the positive ε set for Method 1. The probabilities of collapse associated with the 2% in 50 years motion are similar (0.5 and 2.4%), and when the collapse CDF is integrated with the site hazard curve for the example site, the mean annual rates of collapse λ_{col} differ only by a factor of 2, as shown in Fig. 9. These differences are negligible when compared to a factor of 23 in the overprediction of λ_{col} that results from not accounting for the proper ε . In addition, data from Haselton and Deierlein (2007, chapter 6) show that even minor differences in the structural design can cause the λ_{col} prediction to change by a factor of 1.5–2.2, which is similar to the difference in results from the two methods compared here.

Simplified Method to Account for Effects of Epsilon

Motivation and Overview

The preceding section showed that we can obtain roughly the same collapse capacity predictions by either (a) selecting records with appropriate ε values (Method 1) or (b) using general ground motions and then applying a correction factor to account for the appropriate ε (Method 2). Method 2 is useful because it can account for the target ε without needing to select a unique ground-motion set for each building period and site. However, as described in the preceding section, Method 2 requires a significant effort to compute $\varepsilon(T_1)$ values for each ground-motion record and then to perform a regression analysis to relate $S_{a,col}(T_1)$ to $\varepsilon(T_1)$. To provide a more practical method for adjusting the collapse capacity, a simplified version of Method 2 can be used to determine the appropriate adjustment factors for the collapse capacity distribution without requiring the computation of the $\varepsilon(T_1)$ values for each record and then performing a regression analysis. The simplified method uses an empirical equation to estimate β_1 from Eq. (2) and an approximate value of $\sigma_{LN[Sa,col(T_1)]}$ to correct the collapse capacity distribution.

Building Case Studies to Develop the Simplified Method for ε Adjustment

The complete Method 2 was applied to three sets of RC frame buildings, a total of 111 buildings, to develop a simplified adjustment approach. They included:

- Sixty-five modern RC SMF buildings ranging in height from 1–20 stories. Thirty of these buildings were code-conforming buildings that were representative of current design [ASCE 7-05 (ASCE 2005) and ACI 318-05 [American Concrete Institute (ACI) 2005]] in high seismic regions of California

Table 2. Comparison of Collapse Risks for the Example 8-Story RC SMF Building, Predicted by Using the Two Proposed Methods and without Treatment of ε

Method	Mean $S_{a,col}$ (1.71 s)	σ_{LN} (Sa,col)	$P[C S_{a/50}]$	λ_{col} [10^{-4}]
Method 1	1.15	0.28	0.005	0.28
Method 2	1.20	0.38	0.024	0.50
Predictions without ε adjustment	0.72	0.45	0.29	6.3
Ratio: Method 2 to Method 1	1.0	1.2	5	2
Ratio: Without adjustment to Method 1	0.63	1.6	58	23

Table 3. Results for a Subset of the 111 Buildings Showing the Relationship between Building Deformation Capacity RDR_{ult} and β_1 , a Measure of the Significance of $\varepsilon(T_1)$ in Collapse Capacity Predictions in which β_1 Is Obtained from Regression Analysis

Design information		RC SMF buildings			1967 RC frame buildings			RC OMF buildings		
Number of stories	Framing system	RDR_{ult}	β_1	$\sigma_{LN,reg}/\sigma_{LN}$	RDR_{ult}	β_1	$\sigma_{LN,reg}/\sigma_{LN}$	RDR_{ult}	β_1	$\sigma_{LN,reg}/\sigma_{LN}$
2	Perimeter	0.067	0.26	0.82	0.035	0.22	0.86	0.024	0.28	0.95
	Space	0.085	0.26	0.81	0.019	0.16	0.91	0.019	0.09	0.97
4	Perimeter	0.038	0.27	0.83	0.013	0.18	0.90	0.016	0.24	0.92
	Space	0.047	0.26	0.83	0.016	0.20	0.88	0.011	0.27	0.97
8	Perimeter	0.023	0.31	0.81	0.007	0.16	0.97	0.009	0.12	0.82
	Space	0.028	0.32	0.79	0.011	0.18	0.95	0.014	0.19	0.95
12	Perimeter	0.026	0.29	0.84	0.005	0.10	0.97	0.009	0.17	0.97
	Space	0.022	0.25	0.86	0.010	0.16	0.95	—	0.16	—
Mean of subset:		0.033	0.27	0.82	0.012	0.17	0.93	0.014	0.18	0.95
Mean of full set:		—	0.28	—	—	0.18	—	—	0.19	—

(Haselton and Deierlein 2007, chapter 6). The other 35 RC SMF buildings (4- and 12-story) were designed to meet revised structural design requirements, including variations to design strength requirements, interstory drifts, and strong column-weak beam ratio (Haselton and Deierlein 2007, chapter 7).

- Twenty code-conforming ordinary moment frame (OMF) buildings ranging from 2–12 stories, which were representative of buildings in the eastern United States. These designs were developed as part of the “Applied Technology Council-63 Project” (FEMA 2008).
- Twenty-six nonductile RC frame buildings, which were representative of existing 1967-era buildings, ranging from 2–12 stories in high seismic regions of California (Liel 2008).

The collapse analysis was conducted for each building and the regression analysis was applied to $\text{LN}[S_{a,col}(T_1)]$ versus $\varepsilon(T_1)$ to determine the factor β_1 as defined in Eq. (2). A selected subset of these values is shown in Table 3. The mean β_1 value for the 65 RC SMF buildings was $\beta_1 = 0.28$. This value is exceptionally stable with a coefficient of variation value of only 0.14 over the wide variety of buildings of varying heights and design. The stability of the β_1 values indicates that the influence of ε (i.e., spectral shape) on the collapse capacity is fairly consistent among buildings with similar levels of inelastic deformation capacity. The mean value for the 20 RC OMF buildings was $\beta_1 = 0.19$, which is 40% lower than the more ductile SMF buildings. The mean value for the 1967-era buildings was $\beta_1 = 0.18$, which is quite similar the

RC OMF frames. The lower β_1 values indicate that ε has less of an influence on the collapse capacities for the RC OMF and the 1967-era RC frame buildings, both of which have less inelastic deformation capacity as compared to the RC SMF buildings. Building deformation capacities, as quantified by the ultimate roof drift ratio, are also reported in Table 3. Note that RDR_{ult} is the roof drift ratio at 20% strength loss, as predicted by using static pushover analysis (e.g., $RDR_{ult} = 0.047$ for the pushover shown in Fig. 13). Table 3 shows that buildings with a larger deformation capacity RDR_{ult} have higher values of β_1 .

Developing Components of the Simplified Method

Prediction of β_1

The significance of ε , as reflected in the β_1 parameter, is larger for buildings with a higher deformation capacity because ductile buildings soften, and their effective period increases before collapse, which makes the spectral shape, specifically spectral values at $T > T_1$, more important to the structural response. The trend between β_1 and RDR_{ult} is illustrated in Fig. 11(a) for four sets of RC SMF buildings, each set with the same height. These data show a trend for deformation capacities up to $RDR_{ult} = 0.04$, and suggest that deformation capacity in excess of this (i.e., $RDR_{ult} > 0.04$) does not influence β_1 .

β_1 also tends to be larger for taller buildings because of the significance of higher mode effects on the dynamic response of tall buildings, thereby making the spectral shape for periods less

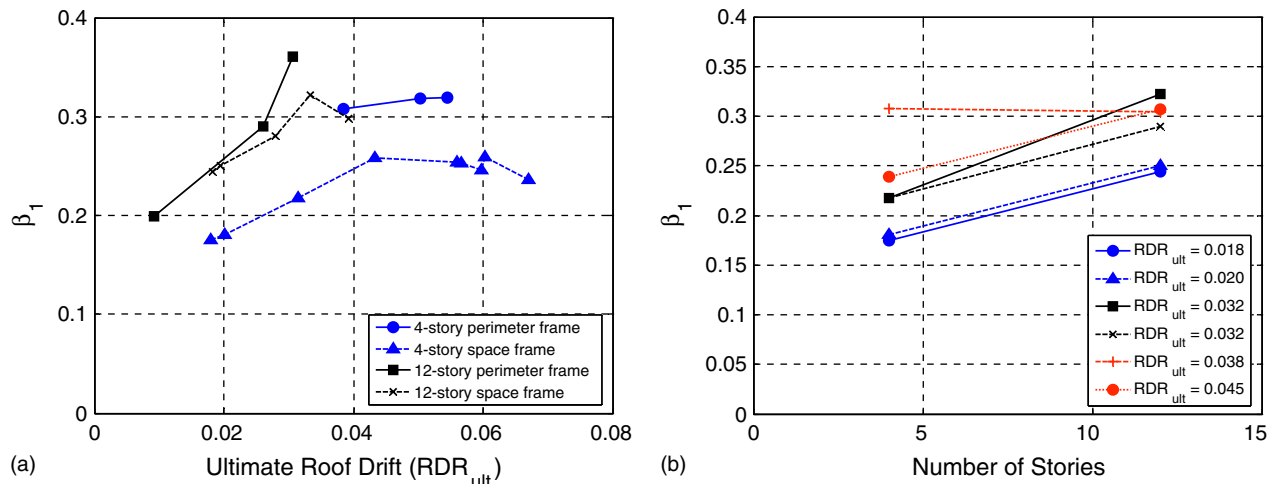


Fig. 11. Relationship between (a) β_1 and building deformation capacity RDR_{ult} ; and (b) β_1 and number of stories

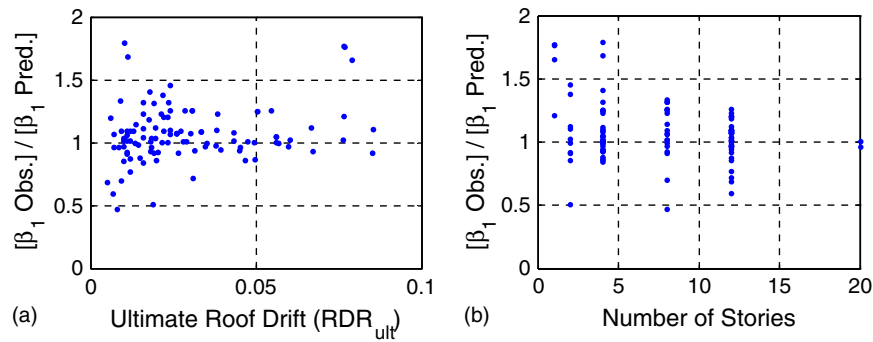


Fig. 12. Ratio of observed/predicted β_1 , plotted against (a) building deformation capacity RDR_{ult} ; and (b) number of stories

than T_1 an important consideration. To investigate the impact of building height, separate from deformation capacity, Fig. 11(b) compares the β_1 values of six pairs of 4- and 12-story RC SMF buildings that have the same RDR_{ult} values. These data show a clear trend between β_1 and building height, for five of the six sets of buildings considered.

Standard linear regression analysis was used to calculate $\text{LN}(\beta_1)$ as a function of RDR_{ult} and building height, on the basis of the data from all 111 buildings to create the predictive equation for β_1 (Chatterjee et al. 2000). We then applied judgmental corrections to better replicate the trends with deformation capacity and building height (see Fig. 11). These corrections were required because of the limited number of data points available to reflect the separate trends of height and building deformation capacity. The functional form of Eq. (8) captures the nearly linear effects of height and the nonlinear effects of RDR_{ult}^* for buildings with a lower deformation capacity. The resulting equation for β_1 becomes

$$\hat{\beta}_1 = (0.4)(N + 5)^{0.35}(RDR_{ult}^*)^{0.38} \quad (8)$$

where N = number of stories limited to $N \leq 20$ on the basis of available data and $RDR_{ult}^* = \text{roof drift ratio at 20\% base shear strength loss from the static pushover analysis}$ [$RDR_{ult}^* = \min(RDR_{ult}, 0.04)$] and the observation from Fig. 11 (a) that the trend saturates at a value of 0.04. Note that the application of static pushover analysis to taller buildings is limited because of the important impact of higher modes, but it is utilized here to approximate the building deformation capacity.

The effects of height and deformation capacity tend to counteract one another, which is why β_1 is fairly consistent for the set of 30 code-conforming RC frame buildings varying from 1 to 20 stories. In Fig. 12, the ratio of observed β_1 to the predicted β_1 from Eq. (8) is plotted against the building deformation capacity and the number of stories, which shows that Eq. (8) provides reasonable predictions for most of the 111 buildings used in this study. However, β_1 is significantly underpredicted (i.e., conservative) for three of the 1-story buildings, but is accurate for the fourth 1-story building. It would be useful to extend this study to include a larger number of short period buildings to further validate the proposed relationship.

Prediction of $\sigma'_{\text{LN}[S_{a,\text{col}}(T_1)]}$

The data in Table 3 show that accounting for ε reduces the dispersion in collapse capacity. This reduction in dispersion is reduced by about 10–15% for ductile RC SMF buildings and 5% for nonductile buildings. For simplicity, it is proposed to ignore this effect and to compute the dispersion directly from the general set, that is, to assume that

$$\sigma'_{\text{LN}[S_{a,\text{col}}(T_1)]} \approx \sigma_{\text{LN}[S_{a,\text{col}}(T_1)]} \quad (9)$$

Proposed Simplified Method

This section summarizes the proposed simplified method for adjusting the collapse capacity to reflect an appropriate spectral shape with an illustration for a 4-story RC SMF space frame.

1. Build a structural model that is robust and able to simulate structural collapse. Calculate the building period and perform a static pushover analysis with a reasonable load pattern to determine the roof drift ratio RDR_{ult} at 20% of lateral strength loss. For this example a 4-story RC SMF building, $T_1 = 0.94$ s. Calculations for the static pushover analysis were conducted by using the lateral load pattern recommended by ASCE 7-05 (ASCE 2005) resulting in the pushover curve shown in Fig. 13 where $RDR_{ult} = 0.047$.
2. Perform nonlinear dynamic analyses to predict the collapse capacity by using the FEMA P695 (FEMA 2008) far-field set of 44 records. [Alternatively, one could use the larger general set of 78 records. However, our analyses have shown that the two sets result in nearly identical mean and dispersion of collapse capacity. The reason for using the larger set in this paper was to better predict the regression line between $\text{LN}[S_{a,\text{col}}(T_1)]$ and $\varepsilon(T_1)$; this additional information is not required in the simplified method.] Compute the natural logarithm of the collapse capacity for each record, and then compute the mean and the standard deviation of these values for all records (i.e., $\mu_{\text{LN}[S_{a,\text{col}}(T_1)]}$ and $\sigma_{\text{LN}[S_{a,\text{col}}(T_1)]}$). For the example 4-story RC SMF building, the results of the nonlinear dynamic collapse analyses are shown as follows:

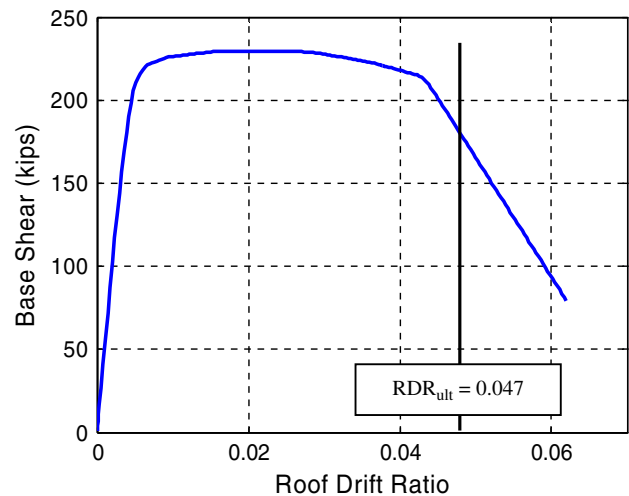


Fig. 13. Static pushover curve for an example 4-story RC SMF building (ID 1008)

$$\mu_{\text{LN}[\text{Sa, col}(T_1)]} = \mu_{\text{LN}[\text{Sa, col}(0.94 \text{ s})]} = 0.601 \quad (10)$$

$$\sigma_{\text{LN}[\text{Sa, col}(T_1)]} = \sigma_{\text{LN}[\text{Sa, col}(0.94 \text{ s})]} = 0.40 \quad (11)$$

The mean collapse capacity can be computed from the logarithmic mean as follows:

$$\text{Mean}_{[\text{Sa, col}(0.94 \text{ s})]} = \exp\{\mu_{\text{LN}[\text{Sa, col}(0.94 \text{ s})]}\} = 1.82 \text{ g} \quad (12)$$

3. Estimate β_1 by using Eq. (8). For the 4-story RC SMF example

$$\hat{\beta}_1 = (0.4)(N + 5)^{0.35} (\text{RDR}_{\text{ult}}^*)^{0.38} \quad (13)$$

$$\text{RDR}_{\text{ult}}^* = 0.04 \quad (14)$$

$$\hat{\beta}_1 = (0.4)(4 + 5)^{0.35} (0.04)^{0.38} = 0.254 \quad (15)$$

4. Determine the target mean ε value $\varepsilon(T_1)_{\text{target}}$ for the site and hazard level of interest. For the example 4-story RC SMF, we assumed that the target is $[\varepsilon(T_1)_{\text{target}}] = 1.9$, which is similar to an expected ε value of a 2% in 50 years ground-motion level in Riverside, California (see Table 1).
5. Adjust for the difference between the target ε value and the ε values of the ground motions used in the collapse simulation. To do this, the mean ε value from the general set of records $\bar{\varepsilon}(T_1)_{\text{records}}$ is required. The mean ε values for the general set of records is shown in Fig. 14. From this figure, one can read the value of $\bar{\varepsilon}(T_1)_{\text{records}}$. For the example building $T_1 = 0.94 \text{ s}$, and because the collapse simulation is calculated by using the 78 general record set, $\bar{\varepsilon}(T_1)_{\text{records}} = 0.17$. Any set of ground motions could be used provided that $\bar{\varepsilon}(T_1)_{\text{records}}$ is known.
6. Compute the adjusted mean collapse capacity. This adjusted capacity accounts for the difference between the mean ε of the general set of records $\bar{\varepsilon}(T_1)_{\text{records}}$ and the target ε values

that come from disaggregation $\bar{\varepsilon}_0(T_1)$. The following equations illustrate this calculation for the example 4-story RC SMF

$$\mu'_{\text{LN}[\text{Sa, col}(T_1)]} = \mu_{\text{LN}[\text{Sa, col}(T_1)]} + \hat{\beta}_1 [\bar{\varepsilon}_0(T_1) - \bar{\varepsilon}(T_1)_{\text{records}}] \quad (16)$$

$$\begin{aligned} \mu'_{\text{LN}[\text{Sa, col}(0.94 \text{ s})]} &= 0.601 + 0.254(1.9 - 0.17) \\ &= 1.040 \end{aligned} \quad (17)$$

$$\begin{aligned} \text{Mean}'_{\text{Sa, col}(0.94 \text{ s})} &= \exp\{\mu'_{\text{LN}[\text{Sa, col}(0.94 \text{ s})]}\} = \exp(1.040) \\ &= 2.83 \text{ g} \end{aligned} \quad (18)$$

The ratio of the adjusted to unadjusted mean collapse capacity can also be computed by using Eqs. (12) and (18), as follows:

$$\begin{aligned} \text{Ratio} &= \frac{\text{Mean}'_{\text{Sa, col}(T_1)}}{\text{Mean}_{[\text{Sa, col}(T_1)]}} = \frac{\text{Mean}'_{\text{Sa, col}(0.94 \text{ s})}}{\text{Mean}_{[\text{Sa, col}(0.94 \text{ s})]}} = \frac{2.83 \text{ g}}{1.82 \text{ g}} \\ &= 1.55 \end{aligned} \quad (19)$$

7. Compute the dispersion in the collapse capacity by using Eq. (10). In this step, we propose to simply use the value computed directly from the nonlinear dynamic analyses, where

$$\sigma'_{\text{LN}[\text{Sa, col}(T_1)]} \approx \sigma_{\text{LN}[\text{Sa, col}(T_1)]} = 0.40 \quad (20)$$

Comparison of the Simplified Method and Method 2

For comparison, applying Method 2 to this same building by using data from Haselton and Deierlein (2007, chapter 3) would result in very similar results to the Simplified Method. The full regression analysis results yield $\beta_1 = 0.257$, which agrees very well with the simplified value of $\hat{\beta}_1 = 0.254$. The corresponding mean collapse capacity from Method 2 is 2.63 g as compared to the simplified value of 2.83 g. This difference of about 8% is reasonable for most applications, particularly in contrast to the alternative of neglecting

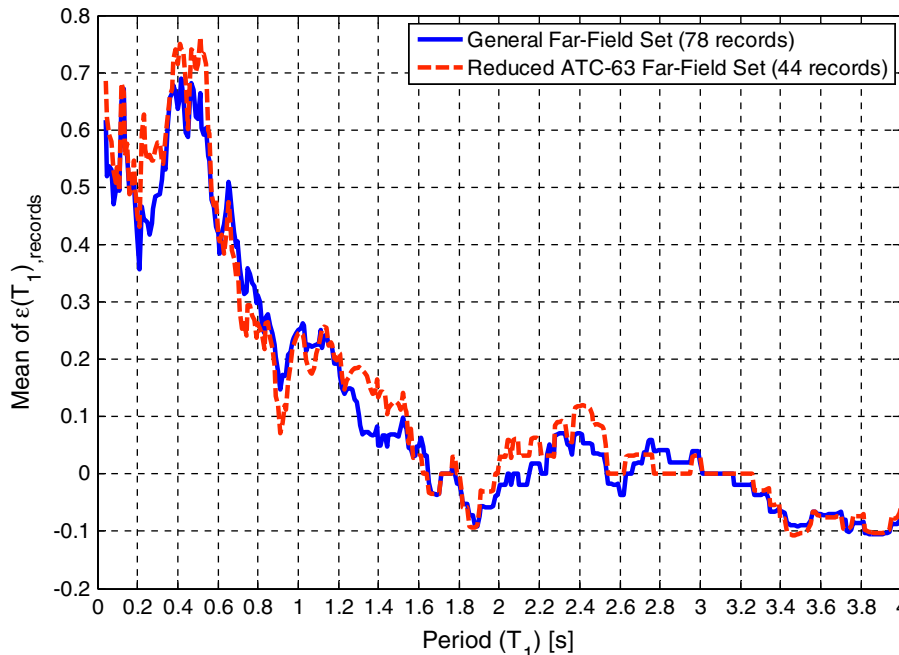


Fig. 14. Mean ε values for the full and reduced versions of general set of ground motions $\bar{\varepsilon}(T_1)_{\text{records}}$

the spectral shape effects. The calculated dispersion from Method 2 is $\sigma'_{\text{LN}[S_{a,\text{col}}(T_1)]} = 0.35$, which is about 10% lower than the slightly conservative value of 0.40 used in the simplified method. The conditional probability of collapse for the 2% in 50 years ground-motion level $S_a(0.94 \text{ s}) = 0.87 \text{ g}$ is effectively zero in both cases, 0.2% and 0.1%, respectively.

Summary, Limitations, and Future Work

The consideration of spectral shape is critical in the selection and scaling of ground motions for use in a collapse assessment by nonlinear dynamic analysis. This paper presents that the spectral shape characteristics can be included in a collapse assessment through consideration of the parameter ε , which is a measure of how ground-motion acceleration spectra vary from the mean predictions provided by ground-motion attenuation relationships. For an example 8-story RC SMF building, accounting for the ε adjustment increased the mean collapse capacity by a factor of 1.6, decreased the conditional probability of collapse for the 2% in 50 years ground motion, $P[C|S_{a2/50}]$, from 29% to 0.5%, and decreased the mean annual frequency of collapse by a factor of 23.

The most direct approach to account for the ε -effect in collapse assessment is to select ground motions whose $\varepsilon(T_1)$ values match those of the building site, the collapse intensity S_a , and the structural period of interest. However, this approach is often impractical and sometimes infeasible when assessing the collapse performance of buildings with varying vibration periods at multiple sites and under varying ground-motion intensities. An alternative simplified approach is proposed that applies an adjustment to the collapse capacity by using the target $\varepsilon(T_1)$, which eliminates the necessity of considering $\varepsilon(T_1)$ in the selection of the ground-motion records. Two variants of the ε -adjustment method are proposed, one of which is a simplified version of the other.

To develop and validate the proposed ε -adjustment method, the collapse capacities of three sets of RC frame buildings were investigated including (a) 65 modern RC ductile special moment frames, (b) 26 nonductile 1967-era RC frames, and (c) 20 RC limited-ductility ordinary moment frames. These 111 buildings range in height from 1–20 stories with fundamental vibration periods ranging from 0.4–4.4 s, with most periods less than 3.0 s. We simulated the collapse capacity of each building for 78 ground-motion records, and then used regression analysis to find the relationship between the collapse intensity $S_{a,\text{col}}(T_1)$ and the corresponding $\varepsilon(T_1)$ for each building and ground motion. The resulting collapse capacities calculated through this regression technique, called Method 2 in this paper, are shown to agree well with the results obtained by using a ground-motion set selected to have the target ε .

A simplified version of Method 2 was developed, in which a semiempirical equation [Eq. (8)] was used to calculate the $\varepsilon(T_1)$ collapse adjustment factor in lieu of conducting regression analyses. Generalized regression analyses conducted by using data from the collapse capacities of the 111 case study buildings were used to develop this equation. The resulting semiempirical equation [Eq. (8)] reflects variations in building height and deformation capacity, the latter of which is determined by using a pushover analysis. The proposed simplified method allows the analyst to use a general ground-motion set, selected without regard to ε , to calculate an unadjusted building collapse capacity by using nonlinear dynamic analysis, and then to correct this capacity by using an adjustment factor to reflect the expected $\varepsilon(T_1)$ for the building site and collapse hazard intensity, $S_{a,\text{col}}(T_1)$. The general set of far-field strong ground motions from the FEMA P695 (FEMA 2008) are suggested for applying this simplified procedure.

Whereas Method 2 is general in its applicability, the simplified method should be utilized only for structures and ground motions similar to those to which it was developed and calibrated. The development was limited to moment frame buildings, ranging in height from 1 to 20 stories and ranging in periods from 0.4–3.0 s. The ground motions and target ε values used in the study are generally representative of Site Classes B, C, and D, with a focus on ε values in the range of $\varepsilon = 0$ to $+2.0$. The simplified method should not be used for other site classes, particularly soft soil sites, or for sites with target ε values outside of the noted range without appropriate ground-motion selection and recalibration of the adjustment factor for these conditions.

An implicit assumption of the proposed techniques is that the spectral acceleration at the fundamental period of the building, $S_a(T_1)$, is used to scale the ground motions and quantify the collapse intensity. This assumption is fundamental to the definition of the ε adjustment factor. For tall or irregular buildings, there may be multiple dominant periods of response, the effects of which warrant further study. For example, if three periods dominate the structural response of a tall building, perhaps the collapse assessment could be completed once for each of the three periods, and the controlling case could be used.

This work is currently adapted for use in the “ATC-63 Project” (FEMA 2008) to provide codified guidelines and procedures for the collapse capacity prediction of buildings. The goal of the ATC Project is to use the codified collapse prediction procedures to determine the appropriate prescriptive design requirements (e.g., the R factor) for newly proposed structural systems.

This research could also be extended to look more closely at impacts of spectral shape ε on the collapse behavior of short period buildings. Additionally, this method was developed with the primary goal of identifying a generalized collapse assessment to evaluate the relative safety among groups of buildings located on comparable sites. Further work would be useful to extend this method for a case-specific collapse analysis of specific buildings at particular sites. This extension may involve the selection of records to match the target spectral shape directly (Baker and Cornell 2006), including factors such as site class, which may significantly alter the shape.

Acknowledgments

This research was supported primarily by the Earthquake Engineering Research Centers Program of the National Science Foundation under award number EEC-9701568 through the Pacific Earthquake Engineering Research Center (PEER). The research findings were also supported by related studies conducted for the “ATC-63 Project,” which is supported by the Federal Emergency Management Agency. Any opinions, findings, and conclusions or recommendations expressed in this material are those of the writers and do not necessarily reflect those of the National Science Foundation or the Federal Emergency Management Agency.

The writers also acknowledge the contributions of Nico Luco, Stephen Harmsen, and Arthur Frankel of the USGS, who provided the mean $\bar{\varepsilon}_0$ data used in this research; the suggestions and advice of Dr. Charlie Kircher and other members of the “ATC-63 Project;” and the assistance of Jason Chou and Brian Dean in conducting the structural collapse analyses used in this study.

References

- Abrahamson, N. A., and Silva, W. J. (1997). “Empirical response spectral attenuation relations for shallow crustal earthquake.” *Seismol. Res. Lett.*, 68(1), 94–126.

- American Concrete Institute (ACI). (2005). "Building code requirements for structural concrete." *ACI 318-05*, Farmington Hills, MI.
- ASCE. (2005). "Minimum design loads for buildings and other structures." *ASCE 7-05*, Reston, VA.
- Baker, J. W. (2005). "Vector-valued ground motion intensity measures for probabilistic seismic demand analysis." Ph.D. dissertation, Dept. of Civil and Environmental Engineering, Stanford Univ., Stanford, CA.
- Baker, J. W., and Cornell, C. A. (2006). "Spectral shape, epsilon and record selection." *Earthquake Eng. Struct. Dyn.*, 35(9), 1077–1095.
- Baker, J. W., and Cornell, C. A. (2008). "Vector-valued intensity measures for pulse-like near-fault ground motions." *Eng. Struct.*, 30(4), 1048–1057.
- Baker, J. W., and Jayaram, N. (2008). "Correlation of spectral acceleration values from NGA ground motion models." *Earthquake Spectra*, 24(1), 299–317.
- Benjamin, J. R., and Cornell, C. A. (1970). *Probability, statistics, and decision for civil engineers*, McGraw-Hill, New York.
- Boore, D. M., Joyner, W. B., and Fumal, T. E. (1997). "Equations for estimating horizontal response spectra and peak accelerations from western North America earthquakes: A summary of recent work." *Seismol. Res. Lett.*, 68(1), 128–153.
- Chatterjee, S., Hadi, A. S., and Price, B. (2000). *Regression analysis by example*, 3rd Ed., Wiley, New York.
- Goulet, C., et al. (2007). "Evaluation of the seismic performance of a code-conforming reinforced-concrete frame building—From seismic hazard to collapse safety and economic losses." *Earthquake Eng. Struct. Dyn.*, 36(13), 1973–1997.
- Federal Emergency Management Agency (FEMA). (2008). "Recommended methodology for quantification of building system performance and response parameters." *ATC-63 Project 90% Draft Rep.-FEMA P695*, Applied Technology Council, Redwood City, CA.
- Harmsen, S. C. (2001). "Mean and modal ε in the deaggregation of probabilistic ground motion." *Bull. Seismol. Soc. Am.*, 91(6), 1537–1552.
- Harmsen, S. C., Frankel, A. D., and Petersen, M. D. (2002). "Deaggregation of U.S. seismic hazard: The 2002 update." *USGS Open-File Rep. 03-440*, (<http://pubs.usgs.gov/of/2003/ofr-03-440/ofr-03-440.html>) (Sep. 12, 2006).
- Haselton, C. B., and Baker, J. W. (2006). "Ground motion intensity measures for collapse capacity prediction: Choice of optimal spectral period and effect of spectral shape." *Proc., 8th National Conf. on Earthquake Engineering*, Earthquake Engineering Research Institute, Oakland, CA.
- Haselton, C. B., and Deierlein, G. G. (2007). "Assessing seismic collapse safety of modern reinforced concrete frame." *PEER Rep. 2007/08*, Pacific Engineering Research Center, Univ. of California, Berkeley, CA.
- International Code Council. (2003). *2003 Int. building code*, Falls Church, VA.
- Liel, A. B. (2008). "Assessing the collapse risk of California's existing reinforced concrete frame structures: Metrics for seismic safety decisions." Ph.D. dissertation, Dept. of Civil and Environmental Engineering, Stanford Univ., Stanford, CA.
- Pacific Earthquake Engineering Research Center (PEER). (2008). "PEER Next Generation Attenuation (NGA) database." (<http://peer.berkeley.edu/nga/>) (Jul 2008).
- Tothong, P. (2007). "Probabilistic seismic demand analysis using advanced ground motion intensity measures, attenuation relationships, and near-fault effects." Ph.D. dissertation, Dept. of Civil and Environmental Engineering, Stanford Univ., Stanford, CA.
- Vamvatsikos, D., and Cornell, C. A. (2002). "Incremental dynamic analysis." *Earthquake Eng. Struct. Dyn.*, 31(3), 491–514.
- Zareian, F. (2006). "Simplified performance-based earthquake engineering." Ph.D. dissertation, Dept. of Civil and Environmental Engineering, Stanford Univ., Stanford, CA.